Slow sound in matter-wave dark soliton gases

Muzzamal I. Shaukat,[1,2,3,*] Eduardo V. Castro,[2,4] and Hugo Terças[5,†]

[1]*Instituto Superior Técnico, University of Lisbon and Instituto de Telecomunicações, Torre Norte, Avenida Rovisco Pais 1, Lisbon, Portugal*

[2]*CeFEMA, Instituto Superior Técnico, Universidade de Lisboa, Lisbon, Portugal*

[3]*Department of Natural Sciences, University of Engineering and Technology, Lahore (RCET Campus), Pakistan*

[4]*Centro de Física das Universidades do Minho e Porto, Departamento de Física e Astronomia, Faculdade de Ciéncias, Universidade do Porto, Porto, Portugal*

[5]*Instituto de Plasmas e Fusão Nuclear, Instituto Superior Técnico, Lisbon, Portugal*

(Received 1 November 2018; revised manuscript received 29 March 2019; published 9 May 2019)

We demonstrate the possibility of drastically reducing the velocity of phonons in quasi-one-dimensional Bose-Einstein condensates. Our scheme consists of a dilute dark soliton "gas" that provide the trapping for the impurities that surround the condensate. We tune the interaction between the impurities and the condensate particles in such a way that the dark solitons result in an array of *qutrits* (three-level structures). We compute the phonon-soliton coupling and investigate the decay rates of these three-level qutrits inside the condensate. As such, we are able to reproduce the phenomenon of acoustic transparency based purely on matter-wave phononics, in analogy with the electromagnetically induced transparency effect in quantum optics. Thanks to the unique properties of transmission and dispersion of dark solitons, we show that the speed of an acoustic pulse can be brought down to $\sim 5\ \mu$m/s, $\sim 10^3$ times lower than the condensate sound speed. This is a value that greatly underdoes most of the reported studies for phononic platforms. We believe the present work could pave the stage for a new generation of "stopped-sound"-based quantum information protocols.

DOI: 10.1103/PhysRevB.99.205408

I. INTRODUCTION

Electromagnetically induced transparency (EIT) [1] is a quantum interference effect in which the absorption of a weak probe laser, interacting resonantly with an atomic transition, is reduced in the presence of a coupling laser. EIT plays a crucial role in the optical control of slow light [2] and optical storage [3], having been extensively investigated in Λ-, V-, and cascade-type three-level systems [4,5]. This fascinating effect has been experimentally observed in both atoms [6] and semiconductor quantum wells [7]. A major problem in the initial studies of EIT in atomic vapors has to do with the thermal spectral broadening [8,9], smearing out the EIT window. In order to mitigate this issue, researchers have made use of coherent Bose-Einstein condensates (BECs) [10–12]. The association of EIT with light-matter coupling can be used to prepare and detect coherent many-body phenomena in ultracold quantum gases [13].

Soon after the engineering of photonic crystal structures, attention was drawn to the propagation of acoustic waves in periodic media [14,15]. Many intriguing phenomena, such as the analog of EIT [16,17] and Fano resonances [18,19], have been envisaged in the context of acoustics as well [20,21]. For example, an isotropic metamaterial consisting of grooves on a square bar traps acoustic pulses due to strong modulation of wave group velocity [22]; slowing down the speed of sound in sonic crystal waveguides has also been achieved, with a reported group velocity of 26.7 m/s [23]. Soliton propagation and soliton-soliton interaction in EIT media were studied by Wadati [24], and the formation of solitons via dark-state polaritons was proposed [25].

Recently, we showed that a dark soliton (DS) qubit in a quasi-one-dimensional (quasi-1D) BEC is an appealing candidate to store quantum information, thanks to its appreciably long lifetimes (∼0.01–1 s) [26]. Moreover, we explored the creation of quantum correlation between DS qubits displaced at appreciably large distances (a few micrometers) [27–29]. Dark soliton qubits thus offer an appealing alternative to quantum optics in solid-state platforms, where information processing involves only phononic degrees of freedom: the quantum excitations on top of the BEC state.

In this paper, we propose to make use of dark solitons to achieve a phenomenon with EIT-like characteristics, the *acoustic transparency* (AT). The active medium is composed of a set of dark soliton *qutrits*, i.e., three-level objects comprising an impurity trapped at the interior of a dark soliton potential. Quantum fluctuations are provided by the BEC acoustic (Bogoliubov) modes or simply phonons (see Fig. 1 for a schematic representation). We start by recalling the conditions under which that qutrit is achievable. Then, the qutrit array is shown to be an open quantum system, where the reservoir is composed by the BEC phonons [30]. We compute the linewidth of each of the qutrit transitions by treating the qutrit-phonon interaction within the Born-Markov approximation. We conclude by computing the dispersion relation of a weak envelope of sound waves and show that its group velocity can be drastically reduced to ∼0.06 mm/s. Our study represents an advance in the direction of "slow-

*muzzamalshaukat@gmail.com

†hugo.tercas@tecnico.ulisboa.pt

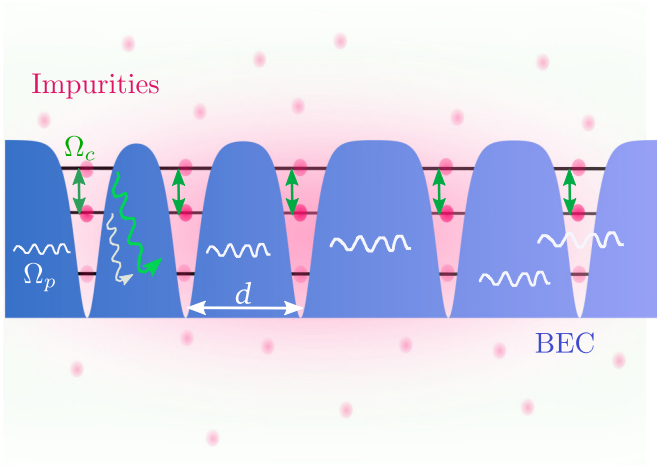

FIG. 1. Schematic representation of dark soliton qutrit array immersed in a BEC. The impurities (free particles) are trapped inside a dark soliton potential. The wiggly lines represent the quantum fluctuations on top of the condensate (phonons).

sound" schemes, and the results have potential applications in phononic information processing.

This paper is organized as follows: In Sec. II, we start with the set of coupled Gross-Pitaevskii and Schrödinger equations to study the properties of dark solitons in a quasi-1D BEC, imprinted on a dilute set of impurities. The coupling between DSs and phonons is computed in Sec. III, followed by a discussion of spontaneous decay of the three-level system in Sec. IV. The concept of slow sound due to the quantum interference phenomenon is described in Sec. V. We conclude the practical implications of the present scheme in Sec. VI.

II. DARK SOLITON QUTRITS

We starting by considering a dark soliton in a quasi-1D BEC, with the latter being surrounded by a dilute gas of impurities (see Fig. 1). The DS plays the role of a potential for the impurities (considered to be free particles), and the phonons act like a quantum (zero-temperature) reservoir. The solitons and the impurities can be treated at the mean-field level, being respectively governed by the Gross-Pitaevskii and Schrödinger equations,

$$\begin{aligned} i\hbar\frac{\partial\psi_1}{\partial t} &= -\frac{\hbar^2}{2m_1}\frac{\partial^2\psi_1}{\partial x^2} + g_{11}|\psi_1|^2\psi_1 + g_{12}|\psi_2|^2\psi_1, \\ i\hbar\frac{\partial\psi_2}{\partial t} &= -\frac{\hbar^2}{2m_2}\frac{\partial^2\psi_2}{\partial x^2} + g_{21}|\psi_{\rm sol}|^2\psi_2. \end{aligned} \tag{1}$$

Here, g_{11} represents the BEC interparticle interaction strength, $g_{12} = g_{21}$ is the BEC-impurity coupling constant (see Appendix A), and m_1 and m_2 denote the BEC particle and impurity masses, respectively. To distinguish the weakly interacting quasi-1D regime from the strongly interacting Tonks-Girandeau gas [31], the dimensionless quantity $\alpha = 2a_s l_z/l_r^2 \ll 1$ is ∼0.06 for BEC and ∼0.07 for impurity particles in the case of dark solitons. Here, l_z (l_r) is the longitudinal (transverse) size, and $a_s \sim$ 0–37 nm is the ^{85}Rb s-wave scattering length [32].

The singular nonlinear solution corresponding to the soliton profile is [33,34]

$$\psi_{\rm sol}(x) = \sqrt{n_0}\tanh\left(\frac{x}{\xi}\right), \tag{2}$$

where n_0 denotes the BEC linear density and $\xi = \hbar/\sqrt{m_1 n_0 g_{11}}$ is the healing length. The latter lies in the range 0.7–1.0 μm in a typical 1D BEC, for which the condensate is homogeneous along a trap of size $L \sim 70\,\mu$m [35]. More recent experiments showed eventual trap inhomogeneities to be much less critical by providing much larger traps, $L \sim 100\,\mu$m [36]. The time-independent version of the impurity equation in (1) reads

$$E'\psi_2 = -\frac{\hbar^2}{2m_2}\frac{\partial^2\psi_2}{\partial x^2} - g_{21}n_0\,\mathrm{sech}^2\left(\frac{x}{\xi}\right)\psi_2, \tag{3}$$

where $E' = E - n_0 g_{21}$ [37]. To find the analytical solution of Eq. (3), the potential is cast in the Pöschl-Teller form $V(x) = -\hbar^2\nu(1+\nu)\mathrm{sech}^2(x/\xi)/2m_2\xi^2$, with $2\nu = -1 + \sqrt{1 + 4g_{21}m_2/g_{11}m_1}$ and the energy spectrum $E'_n = -\hbar^2(\nu - n)^2/2m_2\xi^2$, where n is an integer [38]. The number of bound states created by the DS is $n_{\rm bound} = \lfloor \nu + 1 + \sqrt{\nu(1+\nu)}\rfloor$, where the symbol $\lfloor\cdot\rfloor$ denotes the integer part. As such, for a DS to contain exactly three bound states (i.e., the condition for the qutrit to exist), the parameter ν must lie in the range

$$\tfrac{4}{5} \leqslant \nu < \tfrac{9}{7}. \tag{4}$$

At $\nu \geqslant 9/7$, the number of bound states increases. However, the effect of the impurity on the profile of the soliton itself becomes more important, and therefore, special care must be taken in the choices of the mass ration m_2/m_1. In our numerical calculations below, we choose ^{85}Rb BEC solitons trapping ^{134}Cs impurities (see Appendix A). However, other choices are possible, and our analysis remains general.

III. QUANTUM FLUCTUATIONS

The total BEC quantum field includes the DS wave function and quantum fluctuations, $\psi_1(x) = \psi_{\rm sol}(x) + \delta\psi(x)$, where $\delta\psi(x) = \sum_k [u_k(x)b_k + v_k^*(x)b_k^\dagger]$ and b_k are the bosonic operators verifying the commutation relation $[b_k, b_q^\dagger] = \delta_{k,q}$. The amplitudes $u_k(x)$ and $v_k(x)$ satisfy the normalization condition $|u_k(x)|^2 - |v_k(x)|^2 = 1$ and are explicitly given in Appendix B. The total Hamiltonian then reads $H = H_{\rm q} + H_{\rm p} + H_{\rm int}$, where $H_{\rm q} = \hbar\omega_1(|e_2\rangle\langle e_2| - |e_1\rangle\langle e_1|) + \hbar\omega_0(|e_1\rangle\langle e_1| - |g\rangle\langle g|)$ is the qutrit Hamiltonian, with $\omega_1 = \hbar(2\nu - 3)/(2m\xi^2)$ and $\omega_0 = \hbar(2\nu - 1)/(2m\xi^2)$ being the gap energies for the $|e_2\rangle \leftrightarrow |e_1\rangle$ and $|e_1\rangle \leftrightarrow |g\rangle$ transitions, respectively. The term $H_{\rm p} = \sum_k \epsilon_k b_k^\dagger b_k$ represents the phonon (reservoir) Hamiltonian, where $\epsilon_k = \mu\xi\sqrt{k^2(\xi^2k^2 + 2)}$ is the Bogoliubov spectrum with chemical potential $\mu = g_{11}n_0$. The interaction Hamiltonian is given by

$$H_{\rm int} = g_{12}\int dx\psi_2^\dagger\psi_1^\dagger\psi_1\psi_2, \tag{5}$$

where $\psi_2(x) = \sum_{l=0}^{2} \varphi_l(x) a_l$ describes the impurity field spanned in terms of the bosonic operators a_l, with $\varphi_0(x) = A_0 \mathrm{sech}^{\alpha}(x/\xi)$, $\varphi_1(x) = 2A_1 \tanh(x/\xi)\varphi_0(x)$, and $\varphi_2(x) = \sqrt{2}A_2[1-(1+3\alpha)\tanh^2(x/\xi)]\varphi_0(x)$, where $A_j (j = 0, 1, 2)$ are the normalization constants and $\alpha = \sqrt{2g_{12}m_2/(g_{11}m_1)}$ (see Appendix B). Using the rotating wave approximation (RWA), the first-order perturbed Hamiltonian can be written as

$$H_{\mathrm{int}}^{(1)} = \sum_k \left(g_0^k \sigma_0^+ + g_1^k \sigma_1^+\right) b_k + \left(g_0^{k*} \sigma_0^- + g_1^{k*} \sigma_1^-\right) b_k^\dagger,$$

where $\sigma_{0,1}^+ = a_{e_1,e_2}^\dagger a_{g,e_1}$, $\sigma_{0,1}^- = a_{g,e_1}^\dagger a_{e_1,e_2}$, while the coupling constants $g_{ll'}^k = g_i^k (i = 0, 1)$ are explicitly given in Appendix B. In our RWA calculation, the counterrotating terms proportional to $b_k \sigma_i^-$ and $b_k^\dagger \sigma_i^+$ are dropped. The accuracy of such an approximation can be verified *a posteriori*, provided that the emission rates γ_0 and γ_1 are much smaller than the qutrit transition frequencies ω_0 and ω_1, respectively.

IV. WIGNER-WEISSKOPF THEORY OF SPONTANEOUS DECAY

We employ the Wigner-Weisskopf theory to find the spontaneous decay rate of the states by neglecting the effect of temperature and other external perturbations [39]. In this regard, the qutrit is assumed to be initially at the excited state $|e_2\rangle$, and the phonons are assumed to be in the vacuum state $|0\rangle$. Under such conditions, the wave function of the total system (qutrit + phonons) can be described as

$$|\Phi(t)\rangle = a(t)|e_2, 0\rangle + \sum_k b_k(t)|e_1, 1_k\rangle + \sum_{k,p} b_{k,p}(t)|g, 1_k, 1_p\rangle, \tag{6}$$

where $a(t)$ is the probability amplitude of the excited state $|e_2\rangle$. The qutrit decays to the state $|e_1\rangle$ with probability amplitude $b_k(t)$ by emitting a phonon of wave vector k and frequency ω_k. Subsequently, the qutrit deexcites to the ground state $|g\rangle$ via the emission of a phonon of momentum p, frequency ω_p, and probability amplitude $b_{k,p}(t)$. In the interaction picture, these coefficients can be written as (see Appendix C)

$$\begin{aligned} a(t) &= e^{-\gamma_1 t/2}, \\ b_k(t) &= -i g_0^k \frac{[e^{i(\omega_k-\omega_1)t-\gamma_1 t/2} - e^{-\gamma_0 t/2}]}{i(\omega_k-\omega_1) - \frac{\gamma_1-\gamma_0}{2}}, \\ b_{k,p}(t) &= \frac{g_0^k g_1^k}{i(\omega_k-\omega_1) - \frac{\gamma_1-\gamma_0}{2}} \left[\frac{e^{i(\omega_p-\omega_0)t-\gamma_0 t/2}-1}{i(\omega_p-\omega_0) - \frac{\gamma_0}{2}} \right. \\ &\quad \left. + \frac{1 - e^{i(\omega_k+\omega_p-\omega_0-\omega_1)t-\gamma_1 t/2}}{i(\omega_k+\omega_p-\omega_0-\omega_1) - \frac{\gamma_1}{2}}\right], \end{aligned} \tag{7}$$

where $\gamma_i (i = 0, 1)$ is the ith-state decay rate

$$\gamma_i = \frac{L}{\sqrt{2}\hbar\xi} \int d\omega_k \frac{\sqrt{1+\eta_i}}{\eta_i} |g_i^k|^2 \delta(\omega_k - \omega_i), \tag{8}$$

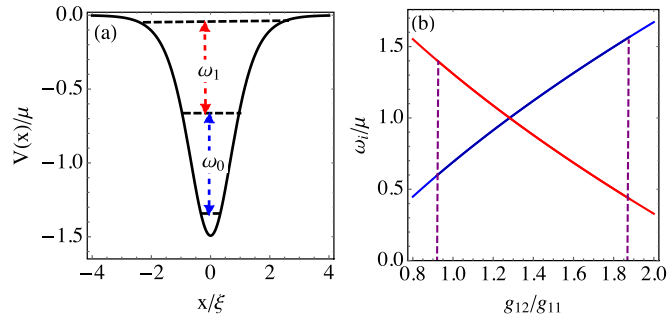

FIG. 2. (a) The impurity states and the respective transition frequencies ω_i $(i = 0, 1)$ in the dark soliton potential. (b) The dependence of the transition frequencies on the BEC-impurity coupling g_{12}. The vertical dashed lines correspond to the range $4/5 \leqslant \nu < 9/7$ defined for the qutrit. For definiteness, we have used $m_2 = 1.56m_1$, corresponding to a ^{134}Cs impurity loaded in a ^{85}Rb BEC dark soliton.

where $\eta_i = \sqrt{\mu^2 + \hbar^2\omega_i^2}$. The validity of both the RWA and the Born-Markov approximations is illustrated in Figs. 2 and 3, which show that the decay rates of both transitions are much smaller than the respective transition frequencies. The soliton retains its shape, which was confirmed by Akram and Pelster [31] while investigating the quasi-1D model of ^{133}Cs impurities in the center of a trapped ^{87}Rb BEC. Moreover, the occurrence of impurity condensation on the bottom of the soliton due to a sufficiently high concentration of impurities leads to the breakdown of the single-particle assumption and a spurious energy shift. This can be avoided if fermionic impurities are used instead [40]. It is pertinent to mention here two experimental considerations. First, notice that Feshbach resonances can be used to tune the value of g_{12}, allowing for an additional control of the rates γ_i. Second, dark soliton quantum diffusion may be the only immediate limitation to the performance of the qutrits [41], a feature that has been theoretically predicted but not yet experimentally validated. In any case, quantum evaporation is expected if important trap anisotropies are present, a limitation that we can overcome with the help of boxlike or ring potentials [35]. This is exactly the situation we will consider in the numerical calculations below.

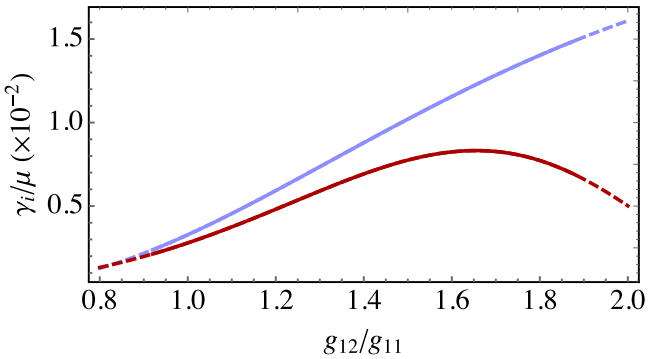

FIG. 3. Dependence of the decay rates γ_0 (blue line) and γ_1 (red line) on the BEC-impurity coupling. The solid lines correspond to the range $\frac{4}{5} \leqslant \nu < \frac{9}{7}$ that defines the qutrit. We have used $m_2 = 1.56m_1$, as in Fig. 7.

V. ACOUSTIC BLOCH EQUATIONS

To produce the interference effect necessary for the AT, we consider the situation where the qutrit is externally driven by two (probe and control) acoustic fields by following the scheme of Raman lasers, described in Refs. [42–44]. The DS qutrit states are coupled to the phonons with a Raman laser driving the transition $|g\rangle \leftrightarrow |e_1\rangle$ with frequency ω_p and detuning $\Delta_p = \omega_p - \omega_0$ to interact with BEC. Simultaneously, a Raman laser field of frequency ω_c and detuning $\Delta_c = \omega_c - \omega_1$ couple the states $|e_1\rangle$ and $|e_2\rangle$. Therefore, the qutrit driving can be described, within the RWA approximation, by the following Hamiltonian:

$$H_{\text{drive}} = \frac{\hbar}{2}(\Omega_p|e_1\rangle\langle g| + \Omega_c|e_2\rangle\langle e_1| - 2\Delta_p|e_1\rangle\langle e_1| - 2\delta|e_2\rangle\langle e_2|) + \text{H.c.}, \tag{9}$$

where $\delta = \Delta_p + \Delta_c$ and $\Omega_{p,c}$ denote the Rabi frequency of the probe and control fields, respectively. We obtain the solution for the density matrix ρ by solving the master equation

$$\dot{\rho_q}(t) = -\frac{i}{\hbar}[H_q, \rho_q(t)] + \sum_{i=0}^{1}\gamma_i\mathcal{L}_i[\rho], \tag{10}$$

with $\rho_{ij} = \rho_{ji}^*$ and the Lindblad operator $\mathcal{L}[\rho] = [\sigma_-\rho_q(t)\sigma_+ - \frac{1}{2}\{\sigma_+\sigma_-, \rho_q(t)\}]$. In the limit of the weak-probe approximation, $\Omega_p \ll \Omega_c$, the steady-state coherences are given by

$$\rho_{21} = \frac{i\Omega_p}{(\gamma_0 - 2i\Delta_p) + \frac{\Omega_c^2}{\gamma_1 - 2i\delta}},$$
$$\rho_{31} = \frac{-i\Omega_c}{(\gamma_1 - 2i\delta)}\rho_{21}. \tag{11}$$

In what follows, we consider a set of solitons, i.e., a soliton gas [45], of density $N = 1/d$, with d denoting the average distance between the solitons. If the solitons are well separated, $d \ll \xi$, we can assume the qutrits are independent. This is not usually the case in one-dimensional systems, unless in the special commensurability situation, as a consequence of the infinite-range (sinusoidal) character of the collective decay rate [46,47]. Fortunately, in our case, because the solitons locally deplete the condensate density, the collective scattering rate vanishes at distances largely exceeding the healing length, $d \gg \xi$ [27,28]. As such, we can determine the long-wavelength behavior, $kd \ll 1$, of the probe field envelope. Using the Heisenberg relation $i\hbar\partial(\delta\Psi)/\partial t = [\hat{H}, \delta\Psi]$ and the fluctuating field $\delta\Psi = \phi b_q e^{iqx} + \psi^* b_q^\dagger e^{-iqx}$, where ϕ and ψ are the Bogoliubov coefficients, we obtain the propagating equation (see Appendix D)

$$\frac{\partial\Omega_p}{\partial t} + \frac{\omega_q}{q}\frac{\partial\Omega_p}{\partial x} = -\frac{i}{2\hbar^2}\left(g_0^{k_{\text{res}}}\right)^2\rho_{12}, \tag{12}$$

where $\Omega_p = N\xi g_0^{k_{\text{res}}}|\delta\Psi|/\hbar$ and $k_{\text{res}} = 0.9/\xi$ is the resonant wave vector. By ignoring the time derivative from Eq. (12) (the time-independent fluctuating field) and comparing it with $\partial_z\delta\Psi = ik\chi\delta\Psi/2$ [48], we express the soliton-gas susceptibility as

$$\chi = -\frac{iN\xi\left(g_0^{k_{\text{res}}}\right)^2}{\hbar\epsilon_k\left[(\gamma_0 - 2i\Delta_p) + \frac{\Omega_c^2}{\gamma_1 - 2i\delta}\right]}, \tag{13}$$

where we have replaced ρ_{12} by its mean value in the soliton gas,

$$\langle\rho_{12}\rangle = \rho_{12}^{\text{gas}} = N\xi\rho_{12},$$

containing the information about the number of solitons per unit length $N\xi$. The acoustic response of the envelope can be determined by the refractive index $n = \sqrt{1+\chi}$. The onset of the AT is demonstrated in Fig. 4. The system initially reveals a normal Lorentzian peak under $\Omega_c \ll \gamma_1$, but a dip appears as we increase the control laser power Ω_c. Moreover, the width of the transparency window increases significantly for $\Omega_c \gg \gamma_1$ and carries a signature of the Autler-Townes doublet. We expect that the destructive interference between the excitation pathways is reduced due to a large value of γ_1. It is important to realize that a change in absorption over a narrow spectral range must be accompanied by a rapid and positive change in the refractive index due to which a very low group velocity is produced in AT. Therefore, the group velocity for the acoustic field is given by

$$v_g = \frac{c_s}{1 + \frac{\chi_R}{2} + \frac{\omega_p}{2}(\partial\chi_R/\partial\omega_p)}, \tag{14}$$

where we assume that $\Omega_c^2 \gg \Gamma_p\Gamma_c$.

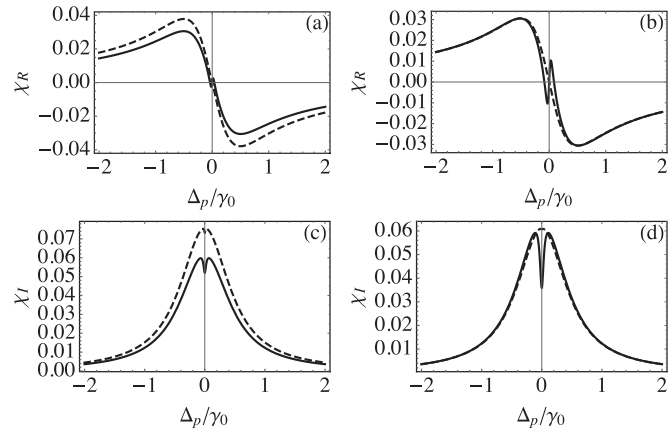

FIG. 4. Acoustic susceptibility χ dependence on the probe detuning Δ_p. (a) The dispersion and (c) absorption spectra calculated for $g_{12} = 1.1g_{11}$ (dashed line) and $g_{12} = 1.85g_{11}$ (solid line), with $\Omega_c > \gamma_1$. (b) The dispersion and (d) absorption for $\Omega_c = 0.2\gamma_0$ (dashed line) and $\Omega_c = 2\gamma_0$ (solid line).

Slow sound in box potentials

For the sake of experimental estimates, we consider a one-dimensional BEC loaded in a large box potential. In a typical trap of size $\sim$100 μm, healing length $\xi \sim 0.7\,\mu$m, and sound speed $c_s \sim 1$ mm/s [35], we can imagine placing up to 20 well-separated ($d \sim 3.5\,\mu$m) solitons. Under these conditions, the envelope group velocity can be brought down to a value of $\sim$0.06 mm/s, corresponding to the peak appearing in Fig. 5. Indeed, for a wavelength compared to an intersoliton

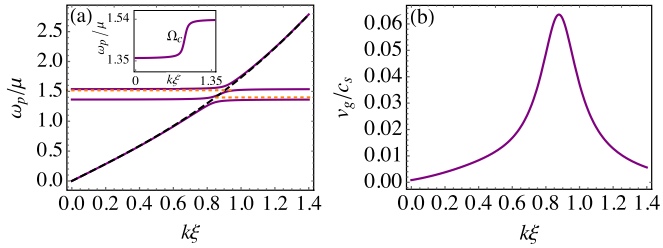

FIG. 5. (a) The dispersion curves, where the solid line illustrates the solutions of Eq. (12) for $g_{12} = 1.85g_{11}$ and the dashed line shows the Bogoliubov energy spectrum. The inset shows the dependence of the absorption (transparency) width on the control Rabi frequency Ω_c. (b) The group velocity v_g of the order of 0.06 of the sound speed c_s. In all cases, we have set $m_2 = 1.56m_1$ and a soliton concentration of $N\xi = 0.2$.

separation d, the estimated group velocity is $v_g \simeq 5.0\,\mu$m/s. This is much smaller than that obtained in band-gap arrays [49] and detuned acoustic resonators [50]. In the latter, a sound speed of ∼9.8 m/s is experimentally reported, which makes our scheme able to produce slow pulses by an $\sim 10^5$ smaller factor.

VI. CONCLUSION

In conclusion, we proposed a scheme for the realization of an acoustic transparency phenomenon with dark soliton qutrits in a quasi-one-dimensional Bose-Einstein condensate, in analogy with the well-known phenomenon of electromagnetically induced transparency. The qutrits consist of three-level structures formed by impurities trapped by the dark solitons. We investigated the spontaneous decay rates to analyze the interference effect of the acoustic transparency, due to which a narrow absorption window, depending on the BEC-impurity coupling, can be achieved. We showed that an acoustic pulse can be slowed down to a speed of $5.0\,\mu$m/s. We believe that the suggested approach opens a promising research avenue in the field of acoustic transport. In general, the present scheme will motivate numerous applications based on the concept of slow or stopped sound, such as quantum memories and quantum information processing [51,52].

ACKNOWLEDGMENTS

This work is supported by the IET under the A. F. Harvey Engineering Research Prize, by FCT/MEC through national funds, and by the FEDER-PT2020 partnership agreement under project UID/EEA/50008/2019. The authors also acknowledge support from Fundação para a Ciência e a Tecnologia (FCT, Portugal), through Grants No. SFRH/PD/BD/113650/2015 and No. IF/00433/2015. E.V.C. acknowledges partial support from FCT through Grant No. UID/CTM/04540/2013.

APPENDIX A: TRAPPING IMPURITIES WITH DARK SOLITONS

We consider a dark soliton in a quasi-1D BEC, which in turn is surrounded by a dilute set of impurities (see Fig. 1 of the main text). The BEC and the impurity particles are described by the wave functions $\psi_1(x,t)$ and $\psi_2(x,t)$, respectively. At the mean-field level, the system is governed by the Gross-Pitaevskii and Schrodinger equations, respectively,

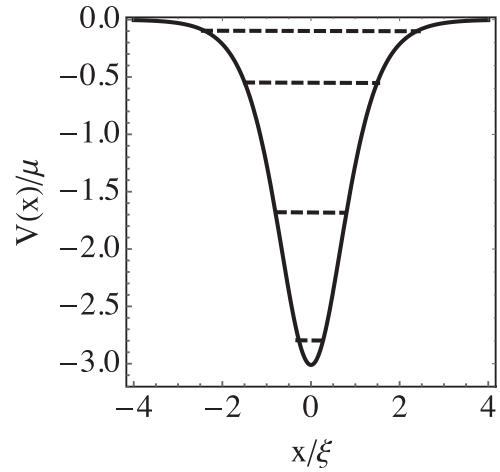

FIG. 6. Schematic representation of a four-level system obtained for $\nu = 10/7$. The highest excited state exists at the border of the potential created by the dark soliton.

$$i\hbar\frac{\partial\psi_1}{\partial t} = -\frac{\hbar^2}{2m_1}\frac{\partial^2\psi_1}{\partial x^2} + g_{11}|\psi_1|^2\psi_1 + g_{12}|\psi_2|^2\psi_1,$$
$$i\hbar\frac{\partial\psi_2}{\partial t} = -\frac{\hbar^2}{2m_2}\frac{\partial^2\psi_2}{\partial x^2} + g_{21}|\psi_1|^2\psi_2. \quad \text{(A1)}$$

Here, the discussion is restricted to repulsive interactions ($g_{11} > 0$) where the dark solitons are assumed to be not significantly disturbed by the presence of impurities, which we consider to be fermionic in order to avoid condensation at the bottom of the potential, and $g_{12} = g_{21}$. To achieve this, the impurity gas is chosen to be sufficiently dilute, i.e., $|\psi_1|^2 \gg |\psi_2|^2$. Such a situation can be produced, for example, by taking ^{134}Cs impurities in a ^{85}Rb BEC [53]. Therefore, the impurities can be regarded as free particles that feel the soliton as a potential,

$$i\hbar\frac{\partial\psi_2}{\partial t} = -\frac{\hbar^2}{2m_2}\frac{\partial^2\psi_2}{\partial x^2} + g_{21}|\psi_{\rm sol}|^2\psi_2, \quad \text{(A2)}$$

where the singular nonlinear solution corresponding to the soliton profile is $\psi_{\rm sol}(x) = \sqrt{n_0}\tanh[x/\xi]$. The time-independent version of Eq. (A2) reads

$$(E - g_{21}n_0)\psi_2 = -\frac{\hbar^2}{2m_2}\frac{\partial^2\psi_2}{\partial x^2} - g_{21}n_0\,\mathrm{sech}^2\left(\frac{x}{\xi}\right)\psi_2. \quad \text{(A3)}$$

To find the analytical solution of Eq. (A3), the potential is cast in the Pöschl-Teller form

$$V(x) = -\frac{\hbar^2}{2m_2\xi^2}\nu(\nu+1)\,\mathrm{sech}^2\left(\frac{x}{\xi}\right), \quad \text{(A4)}$$

with $\nu = (-1 + \sqrt{1 + 4g_{21}m_2/g_{11}m_1})/2$. The particular case of ν being a positive integer belongs to the class of *reflectionless* potentials [38], for which an incident wave is totally transmitted. For the more general case considered here, the energy spectrum associated with the potential in Eq. (A4)

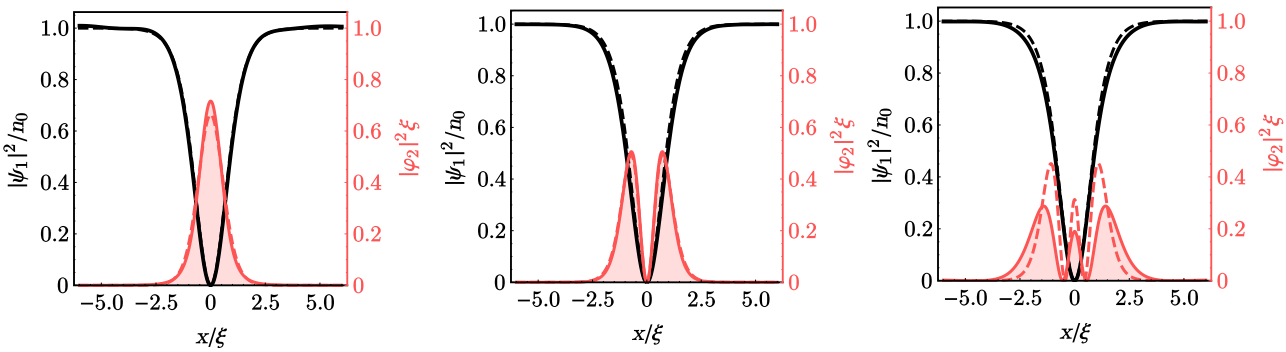

FIG. 7. Qutrits in a possible experimental situation: numerical profiles of the dark soliton (black lines) and the impurity eigenstates (red lines). From left to right, we depict the ground state $\varphi_0(x)$ and the first and second states, $\varphi_1(x)$ and $\varphi_2(x)$, respectively, of a fermionic ^{134}Cs impurity trapped in a ^{85}Rb BEC dark soliton. The solid lines are the numerical solutions, while the dashed lines are the analytical expression described in the main text. We have used the following parameters: $m_2 = 1.56m_1$, $g_{12} = 1.25g_{11}$ (corresponding to $\nu = 1.13$). We fix the number of depleted condensate atoms by the dark soliton to be $n_0\xi \simeq 50$.

reads

$$E_n^{'} = -\frac{\hbar^2}{2m_2\xi^2}(\nu - n)^2, \tag{A5}$$

where n is an integer. The number of bound states created by the dark soliton is $n_{\text{bound}} = \lfloor \nu + 1 + \sqrt{\nu(1+\nu)} \rfloor$, where the symbol $\lfloor\cdot\rfloor$ denotes the integer part. As such, the condition for *exactly* three bound states (i.e., the condition for the qutrit to exist) is obtained if ν sits in the range

$$\frac{4}{5} \leqslant \nu < \frac{9}{7}, \tag{A6}$$

as discussed in the main text. At $\nu \geqslant 9/7$, the number of bound states increases (see Fig. 6 for a schematic illustration).

In Fig. 7, we compare the analytical estimates with the full numerical solution of Eqs. (A1) for both the soliton and the qutrit wave functions under experimentally feasible conditions.

APPENDIX B: SOLITON-PHONON HAMILTONIAN

The interaction Hamiltonian is given by

$$H_{\text{int}} = g_{12}\int dx \psi_2^\dagger \psi_1^\dagger \psi_1 \psi_2, \tag{B1}$$

where $\psi_2(x) = \sum_{l=0}^{2}\varphi_l(x)a_l$ describes the qutrit field in terms of the bosonic operators a_n, with $\varphi_0(x) = A_0\text{sech}^\alpha(x/\xi)$, $\varphi_1(x) = 2A_1\tanh(x/\xi)\varphi_0(x)$, and $\varphi_2(x) = \sqrt{2}A_2[1-(1+3\alpha)\tanh^2(x/\xi)]\varphi_0(x)$, where $A_j (j = 0, 1, 2)$ are the normalization constants, given by

$$A_0 = \left(\frac{\sqrt{\pi}\Gamma[\alpha]}{\Gamma\left[\frac{1+2\alpha}{2}\right]}\right)^{-\frac{1}{2}},$$

$$A_1 = \left[2^{2(1+\alpha)}A_0^2\left(\frac{{}_2F_1[\alpha, 2(1+\alpha), 1+\alpha, -1]}{\alpha} - \frac{{}_2F_1[1+\alpha, 2(1+\alpha), 2+\alpha, -1]}{1+\alpha} + \frac{{}_2F_1[2+\alpha, 2(1+\alpha), 3+\alpha, -1]}{2+\alpha}\right)\right]^{-\frac{1}{2}},$$

$$\begin{aligned} A_2 = \Bigg[& 2A_0^2A_1^2\Bigg(\frac{9\alpha}{2(1+\alpha)} + \frac{9\alpha^2}{4(1+\alpha)} + \frac{9\alpha^2\sqrt{\pi}(6+5\alpha+\alpha^2)\Gamma[\alpha]}{16\Gamma\left[\frac{5}{2}+\alpha\right]} \\ & + \frac{3\times 2^{2(1+\alpha)}\alpha(2+3\alpha){}_2F_1[1+\alpha, 2(2+\alpha), 2+\alpha, -1]}{1+\alpha} + \frac{4^{(2+\alpha)}{}_2F_1[2+\alpha, 2(2+\alpha), 3+\alpha, -1]}{2+\alpha} \\ & + \frac{3\times 2^{2(2+\alpha)}\alpha{}_2F_1[2+\alpha, 2(2+\alpha), 3+\alpha, -1]}{2+\alpha} + \frac{27\times 4^{(1+\alpha)}\alpha^2{}_2F_1[2+\alpha, 2(2+\alpha), 3+\alpha, -1]}{2(2+\alpha)} \\ & + \frac{3\times 2^{(3+2\alpha)}\alpha{}_2F_1[3+\alpha, 2(2+\alpha), 4+\alpha, -1]}{3+\alpha} + \frac{9\times 2^{2(1+\alpha)}\alpha^2{}_2F_1[3+\alpha, 2(2+\alpha), 4+\alpha, -1]}{3+\alpha} \\ & + \frac{9\times 2^{2\alpha}\alpha^2{}_2F_1[4+\alpha, 2(2+\alpha), 5+\alpha, -1]}{4+\alpha}\Bigg)\Bigg]^{-\frac{1}{2}}, \end{aligned} \tag{B2}$$

where ${}_2F_1$ and $\Gamma[\alpha]$ represent the hypergeometric and gamma function, respectively, and $\alpha = \sqrt{2g_{12}/g_{11}}$. The inclusion of quantum fluctuations is performed by writing the BEC field as $\psi_1(x) = \psi_{\text{sol}}(x) + \delta\psi(x)$, where $\delta\psi(x) = \sum_k[u_k(x)b_k + v_k^*(x)b_k^\dagger]$ and b_k are the bosonic operators verifying the commutation relation $[b_k, b_q^\dagger] = \delta_{k,q}$. The amplitudes $u_k(x)$ and $v_k(x)$

satisfy the normalization condition $|u_k(x)|^2 - |v_k(x)|^2 = 1$ and are explicitly given by [41],

$$u_k(x) = \sqrt{\frac{1}{4\pi\xi}}\frac{\mu}{\epsilon_k}\left\{\left[(k\xi)^2 + \frac{2\epsilon_k}{\mu}\right]\left[\frac{k\xi}{2} + i\tanh\left(\frac{x}{\xi}\right)\right] + \frac{k\xi}{\cosh^2\left(\frac{x}{\xi}\right)}\right\}$$

and

$$v_k(x) = \sqrt{\frac{1}{4\pi\xi}}\frac{\mu}{\epsilon_k}\left\{\left[(k\xi)^2 - \frac{2\epsilon_k}{\mu}\right]\left[\frac{k\xi}{2} + i\tanh\left(\frac{x}{\xi}\right)\right] + \frac{k\xi}{\cosh^2\left(\frac{x}{\xi}\right)}\right\}.$$

Using the rotating wave approximation (RWA), the first-order perturbed Hamiltonian can be written as

$$H_{\rm int}^{(1)} = \sum_k \left(g_0^k\sigma_0^+ + g_1^k\sigma_1^+\right)b_k + \left(g_0^{k*}\sigma_0^- + g_1^{k*}\sigma_1^-\right)b_k^\dagger,$$

where $\sigma_{0,1}^+ = a_{e_1,e_2}^\dagger a_{g,e_1}$, $\sigma_{0,1}^- = a_{g,e_1}^\dagger a_{e_1,e_2}$, and the coupling constants $g_{ll'}^k = g_i^k$ $(i = 0, 1)$ are explicitly given by

$$g_0^k = \frac{ig_{12}k^2\xi^{3/2}}{80\epsilon_k}\sqrt{\frac{n_0\pi}{6}}(2\mu + 8k^2\mu\xi^2 + 15\epsilon_k) \times (-4 + k^2\xi^2)\mathrm{csch}\left(\frac{k\pi\xi}{2}\right),$$

$$g_1^k = \frac{ig_{12}k^2\xi^{3/2}}{896\epsilon_k}\sqrt{\frac{n_0\pi}{15}}[28(2k^4\xi^4 - 35k^2\xi^2 + 68)\epsilon_k + \mu(29k^6\xi^6 - 504k^4\xi^4 + 896k^2\xi^2 + 64)]\mathrm{csch}\left(\frac{k\pi\xi}{2}\right).$$

Technically speaking, the RWA approximation here means neglecting the intraband terms in Eq. (B3), whose amplitudes are given by the coefficients g_{ll}^k, illustrated in Fig. 8. This is achieved if we assume that only resonant processes (i.e., phonons with wave vectors k such that their energies ω_k are in resonance with the transitions ω_0 and ω_1, promoting excitation-deexcitation of the impurity inside the soliton) participate in the dynamics. As explained in the main text and as we see below, the validity of our RWA approximation is verified *a posteriori*, holding if the corresponding spontaneous emission rates γ_i $(i = 0, 1)$ are much smaller than the qutrit transition frequencies ω_i.

APPENDIX C: WIGNER-WEISSKOPF THEORY OF SPONTANEOUS DECAY

We employ the Wigner-Weisskopf theory to find the spontaneous decay rate of the states by neglecting the effect of temperature and other external perturbations. This is extremely well justified in our case, as BECs can nowadays be routinely produced well below the critical temperature for condensations. The qutrit is assumed to be initially at the excited state $|e_2\rangle$, and the phonons are assumed to be in the vacuum state $|0\rangle$. Under such conditions, the wave function of the total system (qutrit + phonons) can be described as

$$|\phi(t)\rangle = a(t)|e_2, 0\rangle + \sum_k b_k(t)|e_1, 1_k\rangle + \sum_{k,p} b_{k,p}(t)|g, 1_k, 1_p\rangle, \tag{C1}$$

where $a(t)$ is the probability amplitude of the excited state $|e_2\rangle$. The qutrit decays to the state $|e_1\rangle$ with probability amplitude $b_k(t)$ by emitting a phonon of wave vector k and frequency ω_k. Subsequently, the qutrit deexcites to the ground state $|g\rangle$ via the emission of a q phonon of frequency ω_p and probability amplitude $b_{k,p}(t)$. The Wigner-Weisskopf ansatz (C1) is then let to evolve under the total Hamiltonian in Eq. (B3), for which the corresponding Schrödinger equation yields

$$\begin{aligned}\dot{a}(t) &= -\frac{\gamma_1}{2}a(t),\\ \dot{b}_k(t) &= -\frac{i}{\hbar}g_1^{k*}e^{i(\omega_k-\omega_1)t-\frac{\gamma_1}{2}t} - \frac{\gamma_0}{2}b_k(t),\\ \dot{b}_{k,p}(t) &= -\frac{i}{\hbar}g_0^{p*}b_k(t)e^{i(\omega_p-\omega_0)t},\end{aligned} \tag{C2}$$

which are simplified by following the procedure of Ref. [26]. Here, γ_i $(i = 0, 1)$ is the ith-state decay rate given by

$$\gamma_i = \frac{L}{\sqrt{2}\hbar\xi}\int d\omega_k \frac{\sqrt{1+\eta_i}}{\eta_i}\left|g_i^k\right|^2\delta(\omega_k - \omega_i), \tag{C3}$$

with

$$\gamma_0 = \frac{\pi N_0 g_{12}^2}{76800\hbar\mu^5\xi^2\eta_0\sqrt{\frac{\mu+\eta_0}{\mu}}}(-\mu+\eta_0)(-5\mu+\eta_0)^2\left[8\eta_0 + 3\mu\left(-2 + 5\xi\sqrt{\frac{\hbar^2\omega_0^2}{\mu^2\xi^2}}\right)\right]^2 \times \mathrm{csch}^2\left(\frac{\pi\sqrt{-\mu+\eta_0}}{2\sqrt{\mu}}\right),$$

$$\gamma_1 = \frac{\pi N_0 g_{12}^2}{2.4\times10^7\hbar\mu^7\xi^2\eta_1\sqrt{\frac{\mu+\eta_1}{\mu}}}(-\mu+\eta_1)\left\{-1956\mu^3 + \hbar^2\omega_1^2\left[-591\mu + 56\sqrt{\eta_1^2-\mu^2} + 29\eta_1\right] + 4\mu^2\left[505\eta_1 + 7\sqrt{\frac{\eta_1^2}{\mu^2}-1}(107\mu - 39\eta_1)\right]\right\}^2 \mathrm{csch}^2\left(\frac{\pi\sqrt{-\mu+\eta_1}}{2\sqrt{\mu}}\right),$$

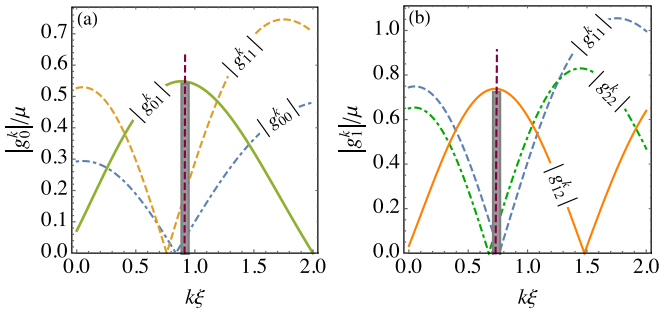

FIG. 8. Interband $g_{ll'}^k$ ($l \neq l'$; solid lines) and intraband $g_{ll'}^k$ ($l = l'$; dashed and dot-dashed lines) coupling amplitudes. Near resonance ($k \sim 0.9\xi^{-1}$ for the first transition and $k \sim 0.7\xi^{-1}$ for the second transition), the interband terms clearly dominate over the intraband transitions, allowing us to neglect the latter within the rotating wave approximation.

where $\eta_i = \sqrt{\mu^2 + \hbar^2\omega_i^2}$. In the long-time limit $t \gg \gamma_i$, Eq. (C2) can be simplified to obtain

$$\begin{aligned} a(t) &= e^{-\gamma_1 t/2}, \\ b_k(t) &= -ig_0^k \frac{[e^{i(\omega_k-\omega_1)t-\gamma_1 t/2} - e^{-\gamma_0 t/2}]}{i(\omega_k-\omega_1) - \frac{\gamma_1-\gamma_0}{2}}, \\ b_{k,p}(t) &= \frac{g_0^k g_1^k}{i(\omega_k-\omega_1) - \frac{\gamma_1-\gamma_0}{2}} \left[\frac{e^{i(\omega_p-\omega_0)t-\gamma_0 t/2} - 1}{i(\omega_p-\omega_0) - \frac{\gamma_0}{2}} \right. \\ &\quad \left. + \frac{1 - e^{i(\omega_k+\omega_p-\omega_{eg})t-\gamma_1 t/2}}{i(\omega_k+\omega_p-\omega_{eg}) - \frac{\gamma_1}{2}} \right], \end{aligned} \tag{C4}$$

where $\omega_{eg} = \omega_0 + \omega_1$, leading to Eq. (7) of the main text.

APPENDIX D: HEISENBERG'S EQUATION AND SOUND PROPAGATION

With the aim of studying how a dilute array of qutrits affects the propagation of sound waves inside the condensate, we compute the equation of motion for a weak acoustic probe coupling the ground and first excited states (i.e., driving the lower transition of the qutrits). This is done with the help of Heisenberg's relation

$$i\hbar \frac{\partial(\delta\Psi)}{\partial t} = [\hat{H}, \delta\Psi], \tag{D1}$$

where $\hat{H} = H_q + H_p + H_{\text{drive}}$ denotes the total Hamiltonian and $\delta\Psi = \phi b_q e^{iqx} + \psi^* b_q^\dagger e^{-iqx}$ is the fluctuating field with the Bogoliubov coefficients ϕ and ψ. Noticing that the commutation relation with the driving Hamiltonian provides

$$[H_{\text{drive}}, \delta\Psi] = \frac{g_0^{k_{res}}}{2\hbar}\rho_{12}, \tag{D2}$$

where $\Omega_p = N\xi g_0^{k_{res}}|\delta\Psi|/\hbar$, and proceeding similarly for the commutation with H_q and H_p, we obtain the following wave equation:

$$\frac{\partial\Omega_p}{\partial t} + \frac{\omega_q}{q}\frac{\partial\Omega_p}{\partial x} = -\frac{i}{2\hbar^2}\left(g_0^{k_{res}}\right)^2\rho_{12}, \tag{D3}$$

corresponding to Eq. (12) of the main text. The quantum interference with the second transition, driven by a coupling field of intensity $\Omega_c \gg \Omega_p$, is contained in the coherence ρ_{12} appearing in the right-hand side of Eq. (D3). The latter can be identified as the acoustic analog of a dynamical susceptibility.

[1] S. E. Harris, J. E. Field, and A. Imamoglu, Phys. Rev. Lett. **64**, 1107 (1990).
[2] L. V. Hau, S. E. Harris, Z. Dutton, and C. H. Behroozi, Nature (London) **397**, 594 (1999).
[3] D. F. Phillips, A. Fleischhauer, A. Mair, R. L. Walsworth, and M. D. Lukin, Phys. Rev. Lett. **86**, 783 (2001).
[4] T. Y. Abi-Salloum, Phys. Rev. A **81**, 053836 (2010).
[5] P. M. Anisimov, J. P. Dowling, and B. C. Sanders, Phys. Rev. Lett. **107**, 163604 (2011).
[6] K.-J. Boller, A. Imamoğlu, and S. E. Harris, Phys. Rev. Lett. **66**, 2593 (1991).
[7] G. B. Serapiglia, E. Paspalakis, C. Sirtori, K. L. Vodopyanov, and C. C. Phillips, Phys. Rev. Lett. **84**, 1019 (2000).
[8] E. A. Cornell and C. E. Wieman, Rev. Mod. Phys. **74**, 875 (2002).
[9] W. Ketterle, Rev. Mod. Phys. **74**, 1131 (2002).
[10] I. Vadeiko, A. V. Prokhorov, A. V. Rybin, and S. M. Arakelyan, Phys. Rev. A **72**, 013804 (2005).
[11] J. G. Ri, C. K. Kim, and K. Nahm, Commun. Theor. Phys. **48**, 461464 (2007).
[12] V. Ahufinger, R. Corbalan, F. Cataliotti, S. Burger, F. Minardi, and C. Fort, Opt. Commun. **211**, 159 (2002).
[13] J. Ruostekoski and D. F. Walls, Phys. Rev. A **59**, R2571 (1999); Eur. Phys. J. D **5**, 335 (1999).
[14] E. Lheurette, *Metamaterials and Wave Control* (Wiley-ISTE, London, 2013).
[15] R. V. Craster and S. Guenneau, *Acoustic Metamaterials: Negative Refraction, Imaging, Lensing and Cloaking*, Springer Series in Metamaterials (Springer, Berlin, 2013), Vol. 166.
[16] N. Liu, L. Langguth, T. Weiss, J. Kästel, M. Fleischhauer, T. Pfau, and H. Giessen, Nat. Mater. **8**, 758 (2009).
[17] M. Fleischhauer, A. Imamoglu, and J. P. Marangos, Rev. Mod. Phys. **77**, 633 (2005).
[18] B. Lukyanchuk, N. I. Zheludev, S. A. Maier, N. J. Halas, P. Nordlander, H. Giessen, and C. T. Chong, Nat. Mater. **9**, 707 (2010).
[19] C. Wu, A. B. Khscianikaev, R. Adato, N. Arju, A. A. Yanik, H. Altug, and G. Shvets, Nat. Mater. **11**, 69 (2011).
[20] A. Santillan and S. I. Bozhevolnyi, Phys. Rev. B **84**, 064304 (2011).
[21] M. Amin, A. Elayouch, M. Farhat, M. Addouche, A. Khelif, and H. Bagci, J. Appl. Phys. **118**, 164901 (2015).
[22] J. Zhu, Y. Chen, X. Zhu, F. J. Garcia-Vidal, X. Yin, W. Zhang, and X. Zhang, Sci. Rep. **3**, 1728 (2013).
[23] A. Cicek, O. A. Kaya, M. Yilmaz, and B. Ulug, J. Appl. Phys. **111**, 013522 (2012).
[24] M. Wadati, Eur. Phys. J. Spec. Top. **173**, 223 (2009).
[25] X. J. Liu, H. Jing, and M. L. Ge, Phys Rev. A **70**, 055802 (2004).

[26] M. I. Shaukat, E. V. Castro, and H. Terças, Phys. Rev. A **95**, 053618 (2017).
[27] M. I. Shaukat, E. V. Castro, and H. Terças, Phys. Rev. A **99**, 042326 (2019).
[28] M. I. Shaukat, E. V. Castro, and H. Terças, Phys. Rev. A **98**, 022319 (2018).
[29] M. I. Shaukat, A. Slaoui, H. Terças, and M. Daoud, arXiv:1903.06627.
[30] L. Pitaevskii and S. Stringari, *Bose-Einstein Condensation* (Clarendon, Oxford, 2003).
[31] J. Akram and A. Pelster, Phys. Rev. A **93**, 033610 (2016).
[32] J. L. Roberts, N. R. Claussen, S. L. Cornish, and C. E. Wieman, Phys. Rev. Lett. **85**, 728 (2000).
[33] V. E. Zakharov and A. B. Shabat, Sov. Phys. JETP **34**, 62 (1972); *ibid.* **37**, 823 (1973).
[34] G. Huang, J. Szeftel, and S. Zhu, Phys. Rev. A **65**, 053605 (2002).
[35] A. L. Gaunt, T. F. Schmidutz, I. Gotlibovych, R. P. Smith, and Z. Hadzibabic, Phys. Rev. Lett. **110**, 200406 (2013).
[36] P. Krüger, S. Hofferberth, I. E. Mazets, I. Lesanovsky, and J. Schmiedmayer, Phys. Rev. Lett. **105**, 265302 (2010).
[37] The present eigenvalue problem can easily be generalized for the case of gray solitons traveling with speed v by replacing $\psi_{\rm sol}(x) = \sqrt{n_0}[i\theta + \gamma \tanh(x\gamma/\xi)]$, where $\theta = v/c_s$ and $\gamma = (1-\theta^2)^{1/2}$. Because this situation is of little use here, we restrict the discussion to only the dark soliton ($v = 0$) case.
[38] J. Lekner, Am. J. Phys. **75**, 1151 (2007).
[39] M. Scully and M. Zubairy, *Quantum Optics* (Cambridge University Press, Cambridge, 1997).
[40] A. H. Hansen, A. Khramov, W. H. Dowd, A. O. Jamison, V. V. Ivanov, and S. Gupta, Phys. Rev. A **84**, 011606 (2011).
[41] J. Dziarmaga, Phys. Rev. A **70**, 063616 (2004).
[42] C. Sabin, A. White, L. Hackermuller, and I. Fuentes, Sci. Rep. **4**, 6436 (2014).
[43] A. Recati, P. O. Fedichev, W. Zwerger, J. von Delft, and P. Zoller, Phys. Rev. Lett. **94**, 040404 (2005).
[44] E. Compagno, G. D. Chiara, D. G. Angelakis, and G. M. Palma, Sci. Rep. **7**, 2355 (2017).
[45] H. Terçaas, D. D. Solnyshkov, and G. Malpuech, Phys. Rev. Lett. **110**, 035303 (2013); **113**, 036403 (2014).
[46] A. Gonzalez-Tudela, D. Martin-Cano, E. Moreno, L. Martin-Moreno, C. Tejedor, and F. J. Garcia-Vidal, Phys. Rev. Lett. **106**, 020501 (2011).
[47] T. Ramos, H. Pichler, A. J. Daley, and P. Zoller, Phys. Rev. Let. **113**, 237203 (2014).
[48] P. Lambropoulos and D. Petrosyan, *Fundamentals of Quantum Optics and Quantum Information* (Springer, Berlin, 2007).
[49] W. M. Robertson, C. Baker, and C. B. Bennett, Am. J. Phys. **72**, 255 (2004).
[50] A. Santillan and S. I. Bozhevolnyi, Phys. Rev. B **89**, 184301 (2014).
[51] H. S. Borges and C. J. Villas-Boas, Phys. Rev. A **94**, 052337 (2016).
[52] O. Lahad and O. Firstenberg, Phys. Rev. Lett. **119**, 113601 (2017).
[53] M. Hohmann, F. Kindermann, B. Gänger, T. Lausch, D. Mayer, F. Schmidt, and A. Widera, EPJ Quantum Technol. **2**, 23 (2015).